Theoretical analyses of the transferred cross-saturation method

Masahiko Matsumoto [a,b], Takumi Ueda [a,b], Ichio Shimada [a,c,*]

[a] *Graduate School of Pharmaceutical Sciences, The University of Tokyo, 7-3-1 Hongo, Bunkyo-ku, Tokyo 113-0033, Japan*
[b] *Japan Biomedicinal Information Research Center (JBIRC), Japan Biological Informatics Consortium (JBIC), 2-3-26 Aomi, Koto-Ku, Tokyo 135-0064, Japan*
[c] *Biological Information Research Center (BIRC), National Institute of Advanced Industrial Science and Technology (AIST), 2-4-7 Aomi, Koto-Ku, Tokyo 135-0064, Japan*

ARTICLE INFO

ABSTRACT

Large molecules, such as membrane proteins, play crucial roles in various biologically important events. We have developed the transferred cross-saturation (TCS) method, which enables the identification of the contact residues of protein ligands in large complexes. However, rational optimization of the experimental conditions for the TCS method has been hampered by the lack of information about the influence of each experimental parameter on the observed TCS effects. Here, we established the theoretical description of the TCS method, which explicitly incorporated the isotopomers in the sample solution, and developed the computer software to perform numerical simulations. Using them, we analyzed the effects of each experimental parameter on the observed TCS effects by the simulations. The simulation studies indicated that: (i) the proton concentration in the solvent should be 10–30%, (ii) a larger p_b, which is the bound fraction of the ligand, is preferred for higher saturation efficiency, (iii) the TCS method is applicable to systems where $k_{off} > 0.1 \text{ s}^{-1}$, (iv) for $k_{off} \geqslant 10 \text{ s}^{-1}$, $p_b \geqslant 0.1$ is preferred, (v) for $k_{off} \sim 1 \text{ s}^{-1}$, $p_b \geqslant 0.5$ is preferred, and (vi) the TCS method is applicable to systems with large τ_c ($\sim 1 \text{ μs}$), where p_b is ~ 0.01. The assumptions in the model spin simulation were experimentally verified, using the ubiquitin–YUH1 interaction. The established method will be useful for estimating and optimizing the TCS experimental conditions.

1. Introduction

Large molecules, such as membrane proteins, play crucial roles in various biologically important events. However, the conventional solution NMR analysis of such large complexes has been hampered by the fast transverse relaxation of their resonances.

We have developed the transferred cross-saturation (TCS) method [1], which enables the identification of the contact residues of protein ligands in large complexes, such as ion channels and their pore blocker peptides [2,3], collagens and collagen-binding proteins [4,5], and liposomes and membrane-permeating antibacterial peptides [6,7]. Similar to the transferred NOE (trNOE) [8,9] and saturation transfer difference (STD) methods [10], the efficiency of the TCS effects depends on various experimental parameters, such as the binding constants between the ligands and the receptors, the molar ratio of the receptors to the ligands, the spatial configurations of the protons in the ligands and the receptors, and the molecular weights of the ligands and the receptors. For the trNOE and STD methods, experimental conditions can be rationally optimized by their theoretical bases and numerical simulations [11–13]. Although these theories form the basis of the TCS method, substantial difficulties are encountered, when they are applied to the TCS method, because each ligand isotopomer in the TCS samples has fairly different spatial configurations of protons (see below).

Here, we established the theoretical description of the TCS method and developed the simulation software. By using the software, we performed the numerical simulation to estimate the effect of each experimental parameter in the TCS method systematically. Based on these results, we demonstrated the applicability of the TCS method and presented the guidelines for the experimental setup.

2. Theory

2.1. Outline of the TCS method

As shown in Fig. 1A, the samples for the TCS experiments consist of non-labeled large molecules ("receptors") and an excess amount of [U–^{2}H,^{15}N] ligand proteins ("ligands") dissolved in the solvent of 10% H_2O/90% D_2O. Under these conditions, the proton densities in the ligand proteins are very low, because the protons in the ligand proteins are all exchangeable and each exchangeable hydrogen site is occupied by ^{1}H at a probability of 10%.
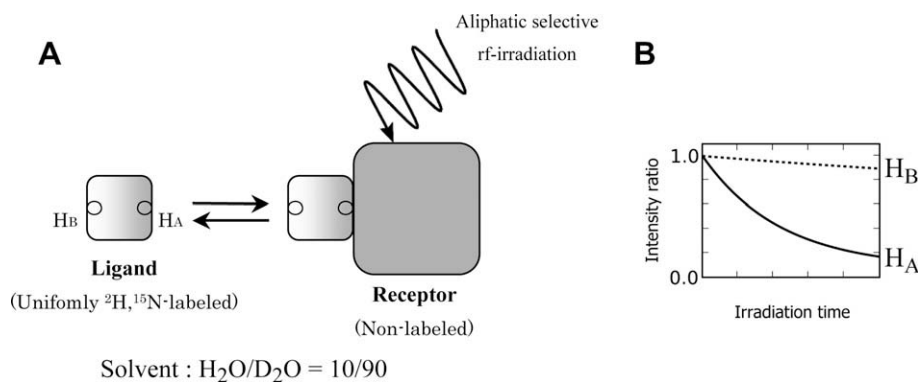
Fig. 1. Schematic diagrams of the transferred cross-saturation (TCS) method. (A) Principle of the transferred cross-saturation (TCS) method. (B) Intensity ratios for proton A, which is in the binding interface, and proton B, which is away from the binding interface.

By irradiating the sample using the radio-frequency (RF) field with the resonant frequency for aliphatic protons, these protons in the receptor molecules are saturated. Since the molecular weight of the receptor is large, the saturation is rapidly transferred to the protons that are not directly irradiated with the RF field in the receptor molecules, such as the aromatic and amide protons. This phenomenon is well known as the spin diffusion effect. The saturation of the receptor protons is also transferred to the protons in the ligand molecules that form complexes with the receptors, through the binding interface. The spin diffusion within the ligand molecules is inefficient, due to the low proton density, and thus the saturation transferred to the ligand molecules is limited to the protons close to the binding interface, typically for up to 2 s of irradiation.

The saturation in the ligand molecules is retained after dissociation, if the complexes have large exchange rates between the free and bound states, such that the longitudinal relaxation time of the ligand protons is longer than the dwell time in the free state of the ligand, as in trNOE and STD methods.

The saturation of the ligand protons in the binding interface is observed as the reductions of their NMR signal intensities in the TCS experiments. Practically, the ^{1}H–^{15}N HSQC spectra are recorded with and without irradiation of the aliphatic protons just before the HSQC pulse sequences, and their signal intensity ratios are calculated. As shown in Fig. 1B, the closer the ligand protons are to the receptor molecules, the larger reduction of the observed signal intensities.

The TCS method is applicable to large protein complexes, for which NMR signals in the complex state are not directly observable, because the NMR signals from the free ligand molecules exchanging between the free and bound states are observed.

2.2. Isotopomers

In standard biomolecular NMR experiments that utilize exchangeable hydrogens in the sample molecules, 5–10% D_2O is added to the solvent for the locking. In such cases, the exchangeable hydrogen sites in the sample molecules are occupied by either ^{1}H or ^{2}H at the probability of the fractional content of protons in the solvents, and therefore, the samples are mixtures of isotopomers. However, these isotopomers are usually neglected, because the spatial configurations of their protons are similar to each other.

In the cross-saturation (CS) or the TCS method, unlike the trNOE and STD methods, the ligand proteins are deuterated and water with a low proton concentration is used as the solvent. Therefore, the spatial configuration of the protons of each isotopomer can be highly varied. The low proton density works to

suppress spin diffusion in the ligand proteins. However, the magnetization behavior in mixtures of isotopomers was not described by the full relaxation matrix treatment in the previous report [14]. Therefore, the observable magnetizations in the CS or TCS methods need to be formulated as an ensemble average of the magnetizations over all of the isotopomers in the sample solution.

2.3. The longitudinal magnetization of each isotopomer during irradiation

Consider a ligand protein that contains n exchangeable hydrogen sites. Out of the 2^n possible isotopomers, we need to treat $2^n - 1$ isotopomers that contain at least one proton. Since the protons in the ligand proteins in the TCS method are all exchangeable, the spatial configuration of the protons in each ligand isotopomer can be highly varied. In contrast, non-labeled receptor molecules contain abundant aliphatic protons, and thus the exchangeable protons have only marginal effects on the spatial configuration of the protons in each receptor isotopomer. For simplicity, we ignore all of the exchangeable hydrogen sites in the receptor molecules, and we assume that the directly irradiated protons are instantaneously saturated.

2.3.1. General theory

The general equation to describe the behavior of the magnetization in the intermolecular saturation transfer experiments in weakly interacting ligand–receptor systems is reported in CORCEMA-ST theory [13]. In the TCS method, the time-course of the longitudinal magnetizations of the protons in the kth isotopomer during the irradiation is given by

$$\frac{d\mathbf{M}_k(t)}{dt} = -(\mathbf{R}_k + \mathbf{K}_k)(\mathbf{M}_k(t) - \mathbf{M}_{0,k}) + \mathbf{Q}_k \qquad (1)$$

where $\mathbf{M}_k(t)$ is a vector consisting of the longitudinal magnetizations of ligand protons and receptor protons that are not directly irradiated, $\mathbf{M}_{0,k}$ is a vector consisting of the magnetizations at thermal equilibrium, $\mathbf{R}_k$ is a relaxation matrix, $\mathbf{K}_k$ is a kinetic matrix, $\mathbf{Q}_k$ is a vector consisting of the sum of the products of the magnetization at thermal equilibrium and the cross relaxation rate constants between the protons that are directly irradiated and the protons that are not directly irradiated, and t is the duration of the irradiation. The 'k' suffixes indicate that the matrices or the vectors are for the kth isotopomer. Eq. (1) can be rewritten with sub-matrices corresponding to the ligand protons and the receptor protons each in the free and bound state, as

$$\frac{d}{dt}\begin{pmatrix}\mathbf{M}_{L_f(k)}(t)\\\mathbf{M}_{R_f}(t)\\\mathbf{M}_{L_b(k)}(t)\\\mathbf{M}_{R_b}(t)\end{pmatrix}=-\left[\begin{pmatrix}\mathbf{R}_{L_f(k)}&\mathbf{0}&\mathbf{0}&\mathbf{0}\\\mathbf{0}&\mathbf{R}_{R_f}&\mathbf{0}&\mathbf{0}\\\mathbf{0}&\mathbf{0}&\mathbf{R}_{L_b(k)}&\mathbf{R}_{L_b(k)R_b}\\\mathbf{0}&\mathbf{0}&\mathbf{R}_{R_bL_b(k)}&\mathbf{R}_{R_b}\end{pmatrix}\right.$$
$$+\left.\begin{pmatrix}k_{on}[R]\mathbf{I}_{L(k)}&\mathbf{0}&-k_{on}[R]\mathbf{I}_{L(k)}&\mathbf{0}\\\mathbf{0}&k_{on}[L]\mathbf{I}_R&\mathbf{0}&-k_{on}[L]\mathbf{I}_R\\-k_{off}\mathbf{I}_{L(k)}&\mathbf{0}&k_{off}\mathbf{I}_{L(k)}&\mathbf{0}\\\mathbf{0}&-k_{off}\mathbf{I}_R&\mathbf{0}&k_{off}\mathbf{I}_R\end{pmatrix}\right]$$
$$\times\begin{pmatrix}\mathbf{M}_{L_f(k)}(t)-\mathbf{M}_{0,L_f(k)}\\\mathbf{M}_{R_f}(t)-\mathbf{M}_{0,R_f}\\\mathbf{M}_{L_b(k)}(t)-\mathbf{M}_{0,L_b(k)}\\\mathbf{M}_{R_b}(t)-\mathbf{M}_{0,R_b}\end{pmatrix}+\begin{pmatrix}\mathbf{0}\\\mathbf{Q}_{R_f}\\\mathbf{Q}_{L_b(k)}\\\mathbf{Q}_{R_b}\end{pmatrix}\qquad(2)$$

where the suffixes '$L_f(k)$', 'R_f', '$L_b(k)$', and 'R_b' indicate the kth isotopomer of the free ligand, the free receptor, the kth isoropomer of the bound ligand, and the bound receptor respectively, $\mathbf{M}_{L_f(k)}(t)$, $\mathbf{M}_{R_f}(t)$, $\mathbf{M}_{L_b(k)}(t)$ and $\mathbf{M}_{R_b}(t)$ are vectors consisting of the magnetizations per unit concentration for the corresponding species, $\mathbf{M}_{0,L_f(k)}$, $\mathbf{M}_{0,R_f}$, $\mathbf{M}_{0,L_b(k)}$ and $\mathbf{M}_{0,R_b}$ are vectors consisting of the magnetizations at thermal equilibrium per unit concentration, $\mathbf{R}_{L_f(k)}$, $\mathbf{R}_{R_f}$, $\mathbf{R}_{L_b(k)}$, and $\mathbf{R}_{R_b}$ are relaxation matrices for the corresponding species, $\mathbf{R}_{L_f(k)R_b}$ and its transpose $\mathbf{R}_{R_bL_f(k)}$ are the off-diagonal elements representing intermolecular cross-relaxation elements, and $\mathbf{Q}_{R_f}$, $\mathbf{Q}_{L_b(k)}$ and $\mathbf{Q}_{R_b}$ are vectors consisting of the products of the magnetization at thermal equilibrium per unit concentration and the cross relaxation rate constants between the protons in the corresponding species and the protons that are directly irradiated, respectively. k_{on} and k_{off} are the second-order association rate constant and the dissociation rate constant, respectively. $[L]$ and $[R]$ are the concentrations of the free ligand and the free receptor, respectively. $\mathbf{I}_{L(k)}$ and $\mathbf{I}_R$ are the identity matrices with the same size as the corresponding block matrix in $\mathbf{R}_k$. Note that all of the magnetizations are defined as values per unit concentration, therefore, the kinetic matrix in Eq. (2) is corrected from the conventional kinetic matrix used in Ref. [13] by multiplying the corresponding concentration ratios, as

$$\mathbf{K}_k=\begin{pmatrix}k_{on}[R]\mathbf{I}_{L(k)}&\mathbf{0}&-k_{off}\mathbf{I}_{L(k)}\times\frac{[LR]}{[L]}&\mathbf{0}\\\mathbf{0}&k_{on}[L]\mathbf{I}_R&\mathbf{0}&-k_{off}\mathbf{I}_R\times\frac{[LR]}{[R]}\\-k_{on}[R]\mathbf{I}_{L(k)}\times\frac{[L]}{[LR]}&\mathbf{0}&k_{off}\mathbf{I}_{L(k)}&\mathbf{0}\\\mathbf{0}&-k_{on}[L]\mathbf{I}_R\times\frac{[R]}{[LR]}&\mathbf{0}&k_{off}\mathbf{I}_R\end{pmatrix}$$
$$=\begin{pmatrix}k_{on}[R]\mathbf{I}_{L(k)}&\mathbf{0}&-k_{on}[R]\mathbf{I}_{L(k)}&\mathbf{0}\\\mathbf{0}&k_{on}[L]\mathbf{I}_R&\mathbf{0}&-k_{on}[L]\mathbf{I}_R\\-k_{off}\mathbf{I}_{L(k)}&\mathbf{0}&k_{off}\mathbf{I}_{L(k)}&\mathbf{0}\\\mathbf{0}&-k_{off}\mathbf{I}_R&\mathbf{0}&k_{off}\mathbf{I}_R\end{pmatrix}\qquad(3)$$

2.3.2. Simplified theory for large receptor systems

If the molecular weight of the receptor is large, then the saturation is efficiently transferred to the protons that are not directly irradiated within the receptor molecules. For simplicity, we assume that all of the protons in the receptor molecules are instantaneously saturated upon irradiation, and thus, the magnetizations of all of the protons in the receptor molecules are assumed to be zero. Therefore, Eq. (2) can be simplified as follows:

$$\frac{d}{dt}\begin{pmatrix}\mathbf{M}_{L_f(k)}(t)\\\mathbf{M}_{L_b(k)}(t)\end{pmatrix}=-\left[\begin{pmatrix}\mathbf{R}_{L_f(k)}&\mathbf{0}\\\mathbf{0}&\mathbf{R}_{L_b(k)}\end{pmatrix}+\begin{pmatrix}k_{on}[R]\mathbf{I}_{L(k)}&-k_{on}[R]\mathbf{I}_{L(k)}\\-k_{off}\mathbf{I}_{L(k)}&k_{off}\mathbf{I}_{L(k)}\end{pmatrix}\right]$$
$$\times\begin{pmatrix}\mathbf{M}_{L_f(k)}(t)-\mathbf{M}_{0,L_f(k)}\\\mathbf{M}_{L_b(k)}(t)-\mathbf{M}_{0,L_b(k)}\end{pmatrix}+\begin{pmatrix}\mathbf{0}\\\mathbf{Q}_{L_b(k)}\end{pmatrix}\qquad(4)$$

The kinetic matrix $\mathbf{K}_k$ in Eq. (4) no longer contains $[L]$, and can be described by k_{off} and the fractional population of the bound ligand, p_b,

$$\mathbf{K}_k=\begin{pmatrix}k_{on}[R]\mathbf{I}_{L(k)}&-k_{on}[R]\mathbf{I}_{L(k)}\\-k_{off}\mathbf{I}_{L(k)}&k_{off}\mathbf{I}_{L(k)}\end{pmatrix}=k_{off}\begin{pmatrix}\frac{p_b}{1-p_b}\mathbf{I}_{L(k)}&-\frac{p_b}{1-p_b}\mathbf{I}_{L(k)}\\-\mathbf{I}_{L(k)}&\mathbf{I}_{L(k)}\end{pmatrix}\qquad(5)$$

For the kth isotopomer of the ligand protein, where n_k out of n exchangeable hydrogen sites are occupied by ^{1}H, $\mathbf{M}_{L_f(k)}(t)$, $\mathbf{M}_{L_b(k)}(t)$, $\mathbf{R}_{L_f(k)}$, $\mathbf{R}_{L_b(k)}$, and $\mathbf{Q}_{L_b(k)}$ in Eq. (4) are given by

$$\mathbf{M}_{L_f(k)}(t)=\begin{pmatrix}M_1^{L_f(k)}(t)\\M_2^{L_f(k)}(t)\\\vdots\\M_{n_k-1}^{L_f(k)}(t)\\M_{n_k}^{L_f(k)}(t)\end{pmatrix}\qquad(6)$$

$$\mathbf{M}_{L_b(k)}(t)=\begin{pmatrix}M_1^{L_b(k)}(t)\\M_2^{L_b(k)}(t)\\\vdots\\M_{n_k-1}^{L_b(k)}(t)\\M_{n_k}^{L_b(k)}(t)\end{pmatrix}\qquad(7)$$

$$\mathbf{R}_{L_f(k)}=\begin{pmatrix}\rho_1^{L_f(k)}&\sigma_{1,2}^{L_f(k)}&\cdots&\sigma_{1,n_k-1}^{L_f(k)}&\sigma_{1,n_k}^{L_f(k)}\\\sigma_{2,1}^{L_f(k)}&\rho_2^{L_f(k)}&\cdots&\sigma_{2,n_k-1}^{L_f(k)}&\sigma_{2,n_k}^{L_f(k)}\\\vdots&\vdots&\ddots&\vdots&\vdots\\\sigma_{n_k-1,1}^{L_f(k)}&\sigma_{n_k-1,2}^{L_f(k)}&\cdots&\rho_{n_k-1}^{L_f(k)}&\sigma_{n_k-1,n_k}^{L_f(k)}\\\sigma_{n_k,1}^{L_f(k)}&\sigma_{n_k,2}^{L_f(k)}&\cdots&\sigma_{n_k,n_k-1}^{L_f(k)}&\rho_{n_k}^{L_f(k)}\end{pmatrix}\qquad(8)$$

$$\mathbf{R}_{L_b(k)}=\begin{pmatrix}\rho_1^{L_b(k)}&\sigma_{1,2}^{L_b(k)}&\cdots&\sigma_{1,n_k-1}^{L_b(k)}&\sigma_{1,n_k}^{L_b(k)}\\\sigma_{2,1}^{L_b(k)}&\rho_2^{L_b(k)}&\cdots&\sigma_{2,n_k-1}^{L_b(k)}&\sigma_{2,n_k}^{L_b(k)}\\\vdots&\vdots&\ddots&\vdots&\vdots\\\sigma_{n_k-1,1}^{L_b(k)}&\sigma_{n_k-1,2}^{L_b(k)}&\cdots&\rho_{n_k-1}^{L_b(k)}&\sigma_{n_k-1,n_k}^{L_b(k)}\\\sigma_{n_k,1}^{L_b(k)}&\sigma_{n_k,2}^{L_b(k)}&\cdots&\sigma_{n_k,n_k-1}^{L_b(k)}&\rho_{n_k}^{L_b(k)}\end{pmatrix}\qquad(9)$$

$$\mathbf{Q}_{L_b(k)}=\begin{pmatrix}\sum_j^{\text{receptor}}\sigma_{1j}^{L_b(k)}M_0\\\sum_j^{\text{receptor}}\sigma_{2j}^{L_b(k)}M_0\\\vdots\\\sum_j^{\text{receptor}}\sigma_{n_k-1,j}^{L_b(k)}M_0\\\sum_j^{\text{receptor}}\sigma_{n_kj}^{L_b(k)}M_0\end{pmatrix}\qquad(10)$$

where $M_i^{L_f(k)}(t)$ and $M_i^{L_b(k)}(t)$ are the longitudinal magnetizations of the ith proton in the kth isotopomer of the ligand in the free and bound states, respectively, $\rho_i^{L_f(k)}$ and $\rho_i^{L_b(k)}$ are the auto-relaxation rate constants of the ith proton in the kth isotopomer of the ligand in the free and bound states, respectively, and $\sigma_{ij}^{L_f(k)}$ and $\sigma_{ij}^{L_b(k)}$ are the cross relaxation rate constants between the ith and jth protons in the kth isotopomer of the ligand in the free and bound states, respectively. $\sum_j^{\text{receptor}}\sigma_{ij}^{L_b(k)}M_0$ is the sum of the cross relaxation rates

between the ith proton in the kth isotopomer of the ligand in the bound state and all of the protons in the receptor molecule.

Under the conditions, where the rotational correlation times are smaller than the reciprocal of the ^{1}H–^{1}H dipole–dipole interactions [15], $\rho_i^{L_f(k)}, \rho_i^{L_b(k)}, \sigma_{ij}^{L_f(k)}$, and $\sigma_{ij}^{L_b(k)}$ are given by

$$\rho_i^{L_f(k)} = R_{1,free}^{DD(^1\mathrm{H})} + R_{1,free}^{DD(^{15}\mathrm{N})} + R_{1,free}^{CSA} \tag{11}$$

$$\rho_i^{L_b(k)} = R_{1,bound}^{DD(^1\mathrm{H})} + R_{1,bound}^{DD(^{15}\mathrm{N})} + R_{1,bound}^{CSA} \tag{12}$$

$$\sigma_{ij}^{L_f(k)} = -d_{HH}^2 \cdot \left(r_{ij}^{(k)}\right)^{-6} \cdot \left\{6J(2\omega_\mathrm{H}, \tau_{c,L}) - J(0, \tau_{c,L})\right\} \tag{13}$$

$$\sigma_{ij}^{L_b(k)} = -d_{HH}^2 \cdot \left(r_{ij}^{(k)}\right)^{-6} \cdot \left\{6J(2\omega_\mathrm{H}, \tau_{c,LR}) - J(0, \tau_{c,LR})\right\} \tag{14}$$

where $r_{ij}^{(k)}$ is the distance between the ith and jth protons in the kth isotopomer of the ligand, and $\tau_{c,L}$ and $\tau_{c,LR}$ are the rotational correlation times of the ligands in the free and bound states, respectively. ω_H is the Larmor frequency of ^{1}H, $d_{HH}^2 = \left(\frac{\mu_0}{4\pi}\right)^2 \frac{\hbar^2 \gamma_\mathrm{H}^4}{10}$, where μ_0 is the vacuum permeability, $\hbar$ is Planck's constant over 2π, γ_H is the gyromagnetic ratio of ^{1}H, and $J(\omega, \tau_c) = \frac{\tau_c}{1+(\omega\tau_c)^2}$. $R_{1,free}^{DD(^1\mathrm{H})}$ and $R_{1,bound}^{DD(^1\mathrm{H})}$ are the longitudinal relaxation rates, due to the ^{1}H–^{1}H dipole–dipole interaction for the free state and bound states, respectively, and are given by

$$R_{1,free}^{DD(^1\mathrm{H})} = d_{HH}^2 \cdot \left\{6J(2\omega_\mathrm{H}, \tau_{c,L}) + 3J(\omega_\mathrm{H}, \tau_{c,L}) + J(0, \tau_{c,L})\right\} \cdot \sum_{j=1, j\neq i}^{n_k} \left(r_{ij}^{(k)}\right)^{-6} \tag{15}$$

$$R_{1,bound}^{DD(^1\mathrm{H})} = d_{HH}^2 \cdot \left\{6J(2\omega_\mathrm{H}, \tau_{c,LR}) + 3J(\omega_\mathrm{H}, \tau_{c,LR}) + J(0, \tau_{c,LR})\right\}$$
$$\cdot \left(\sum_{j=1, j\neq i}^{n_k} \left(r_{ij}^{(k)}\right)^{-6} + \sum_{j}^{receptor} \left(r_{ij}^{(k)}\right)^{-6}\right) \tag{16}$$

$R_{1,free}^{DD(^{15}\mathrm{N})}, R_{1,bound}^{DD(^{15}\mathrm{N})}, R_{1,free}^{CSA}$ and $R_{1,bound}^{CSA}$ are the longitudinal relaxation rates, due to dipole–dipole interactions between bonded ^{1}H and ^{15}N, and the chemical shift anisotropy (CSA) of ^{1}H for the free and the bound states, respectively, and are given by

$$R_{1,free}^{DD(^{15}\mathrm{N})} = d_{HN}^2 \cdot r_{HN}^{-6}$$
$$\cdot \left\{6J(\omega_\mathrm{H}+\omega_\mathrm{N}, \tau_{c,L}) + 3J(\omega_\mathrm{H}, \tau_{c,L}) + J(\omega_\mathrm{H}-\omega_\mathrm{N}, \tau_{c,L})\right\} \tag{17}$$

$$R_{1,bound}^{DD(^{15}\mathrm{N})} = d_{HN}^2 \cdot r_{HN}^{-6}$$
$$\cdot \left\{6J(\omega_\mathrm{H}+\omega_\mathrm{N}, \tau_{c,LR}) + 3J(\omega_\mathrm{H}, \tau_{c,LR}) + J(\omega_\mathrm{H}-\omega_\mathrm{N}, \tau_{c,LR})\right\} \tag{18}$$

$$R_{1,free}^{CSA} = \frac{2}{15}\Delta\sigma_\mathrm{H}^2 \omega_\mathrm{H}^2 J(\omega_\mathrm{H}, \tau_{c,L}) \tag{19}$$

$$R_{1,bound}^{CSA} = \frac{2}{15}\Delta\sigma_\mathrm{H}^2 \omega_\mathrm{H}^2 J(\omega_\mathrm{H}, \tau_{c,LR}) \tag{20}$$

where r_{HN} is the distance between ^{1}H and ^{15}N in the same amide group, ω_N is the Larmor frequency of ^{15}N, and $\Delta\sigma_\mathrm{H}$ is the magnitude of the CSA of amide protons. $d_{HN}^2 = \left(\frac{\mu_0}{4\pi}\right)^2 \frac{\hbar^2 \gamma_\mathrm{H}^2 \gamma_\mathrm{N}^2}{10}$, where γ_N is the gyromagnetic ratio of ^{15}N.

The effects of the exchange with solvents during the irradiation, the dipolar interactions between ^{1}H and ^{2}H, and the internal motions upon relaxation are ignored. Assuming that the initial magnetizations of all of the protons of the ligand proteins are at thermal

equilibrium ($\mathbf{M}_k(0) = \mathbf{M}_{0,k}$), the analytical solution of Eq. (4) is given by

$$\mathbf{M}_k(t) = \mathbf{M}_{0,k} + [\mathbf{I} - \exp\{-(\mathbf{R}_k + \mathbf{K}_k)t\}](\mathbf{R}_k + \mathbf{K}_k)^{-1}\mathbf{Q}_k. \tag{21}$$

where $\mathbf{I}$ is the identity matrix. The observable magnetization in the TCS method is an ensemble average of the magnetizations over all isotopomers. If the molecular weight of the receptor molecule is large, then we can assume that the signals originating from the ligand in the free state are predominantly observed. Under such conditions, the observable magnetization of the proton in the ith exchangeable hydrogen site of the ligand is given by

$$\langle M_i^L(t)\rangle = \overset{\substack{\text{isotopomers}\\\text{containing}\\\text{the }i\text{th proton}}}{\sum_k} p_k M_{i^*}^{L_f(k)}(t) \tag{22}$$

where $M_{i^*}^{L_f(k)}(t)$ is the magnetization of the i^*th proton, which is in the ith hydrogen site, in the kth isotopomer of the ligand in the free state. An asterisk is added to the numbering of the protons in each isotopomer, because the numbering of the protons on each hydrogen site is different among the isotopomers. p_k is the fractional population of the kth isotopomer in the sample solution. Assuming that the H–D exchange reactions with solvents are under equilibrium conditions in all exchangeable hydrogen sites, p_k is given by

$$p_k = p_{proton}^{n_k} \cdot (1 - p_{proton})^{n-n_k} \tag{23}$$

where p_{proton} is the fractional concentration of protons in the sample solvent. The signal intensity for the proton in the ith exchangeable hydrogen site of the ligand, $I_i(t)$, is proportional to $\langle M_i^L(t)\rangle$ and given by

$$I_i(t) = \alpha_i \langle M_i^L(t)\rangle \tag{24}$$

where the coefficient α_i relates the magnitude of the magnetization to the signal intensity for the proton in the ith exchangeable hydrogen site of the ligand. The signal intensity in the reference spectrum, which is recorded without rf-irradiation, is given by

$$I_i(0) = \alpha_i \cdot p_{proton} M_0 \tag{25}$$

The effects of the rf-irradiation in the TCS method are evaluated by the ratio of the signal intensities from spectra recorded with and without irradiation, $I_i(t)/I_i(0)$, which is given by

$$\frac{I_i(t)}{I_i(0)} = \frac{\langle M_i^L(t)\rangle}{p_{proton} M_0} \tag{26}$$

2.3.3. Theory for isolated spin pairs approximation (ISPsA)

In the presence of an extremely low proton concentration, it can be assumed that only ligand isotopomers that contain one proton are predominantly present in the sample solution. Under such conditions, the time-course of the magnetization of each ligand proton is described by 2-coupled differential equations, are given by

$$\frac{d}{dt}\begin{pmatrix} M_f(t) \\ M_b(t) \end{pmatrix} = -\left[\begin{pmatrix} \rho_f & 0 \\ 0 & \rho_b \end{pmatrix} + \begin{pmatrix} k_{+1} & -k_{+1} \\ -k_{-1} & k_{-1} \end{pmatrix}\right]\begin{pmatrix} M_f(t) - M_0 \\ M_b(t) - M_0 \end{pmatrix}$$
$$+ \begin{pmatrix} 0 \\ \sum_i^{receptor} \sigma_i M_0 \end{pmatrix} \tag{27}$$

where $M_f(t)$ and $M_b(t)$ are the magnetizations for the ligand proton in the free and bound states, respectively, ρ_f and ρ_b are the longitudinal relaxation rate constants for the ligand proton in the free and bound states, respectively, $k_{+1} = k_{on}[R]$, and $k_{-1} = k_{off}$. $\sum_i^{receptor}\sigma_i M_0$ is the sum of the intermolecular saturation transfer rates. If we assume that the initial magnetizations of all ligand protons are at a

thermal equilibrium ($M_f(0) = M_b(0) = M_0$), then the analytical solution of Eq. (27) is given by

$$
\begin{pmatrix} M_f(t) \\ M_b(t) \end{pmatrix} = \begin{pmatrix} M_0 \\ M_0 \end{pmatrix}
$$

$$
+ \frac{\sum_i^{\text{receptor}} \sigma_i M_0}{\rho_f \rho_b + \overline{\rho} k_{ex}} \begin{pmatrix} k_{+1}\left(1 + \frac{\lambda_-}{\lambda_+ - \lambda_-} e^{-\lambda_+ t} - \frac{\lambda_+}{\lambda_+ - \lambda_-} e^{-\lambda_- t}\right) \\ \lambda_f - \lambda_- \left(1 - \frac{\lambda_f - \lambda_b}{\lambda_+ - \lambda_-}\right) e^{-\lambda_+ t} - \lambda_+ \left(1 + \frac{\lambda_f - \lambda_b}{\lambda_+ - \lambda_-}\right) e^{-\lambda_- t} \end{pmatrix}
$$

$$(28)$$

where $\quad \lambda_f = \rho_f + k_{+1}, \quad \lambda_b = \rho_b + k_{-1}, \quad k_{ex} = k_{+1} + k_{-1},$ and $\overline{\rho} = (1 - p_b)\rho_f + p_b \rho_b$. λ_+ and λ_- are the eigen values of the dynamic matrix, and are given by

$$
\lambda_\pm = \frac{\rho_f + \rho_b + k_{ex} \pm \sqrt{(\rho_f - \rho_b)^2 + 2(\rho_f - \rho_b)(p_b - p_f)k_{ex} + k_{ex}^2}}{2}
$$

$$(29)$$

if $\rho_f, \rho_b \ll k_{ex}$ (fast exchange on the relaxation time scale), then Eq. (28) can be simplified to

$$
\begin{pmatrix} M_f(t) \\ M_b(t) \end{pmatrix} \approx \begin{pmatrix} M_0 \\ M_0 \end{pmatrix} + \frac{p_b \sum_i^{\text{receptor}} \sigma_i M_0}{\overline{\rho}} \begin{pmatrix} 1 - e^{-\overline{\rho} t} \\ 1 + \frac{p_f \rho_b}{p_b k_{ex}} e^{-k_{ex} t} - e^{-\overline{\rho} t} \end{pmatrix}
$$

$$(30)$$

$M_f(t)$ in Eq. (30) no longer contains k_{off}. The initial slope of $M_f(t)$ in Eq. (30) is given by

$$
\left. \frac{dM_f(t)}{dt} \right|_{t=0} = p_b \sum_i^{\text{receptor}} \sigma_i M_0
$$

$$(31)$$

3. Results and discussion

3.1. Model spin system

To estimate the effects of the experimental conditions in the TCS method, we performed numerical simulations of TCS experiments using a model spin system that mimics large complexes, based on the theories described above. The basic structure of the model spin system used in the present study is shown in Fig. 2A. The ligand consists of three exchangeable protons placed linearly with 3 Å spacing, L1, L2, and L3, and the receptor consists of non-exchangeable protons placed at 3 Å-spaced grid points in a cube. The ligand binds to the center of the receptor cube surface, and the distance from the L1 proton to the closest receptor proton is set to 5 Å. Neither the receptor nor the ligand changes its conformation upon complexation. As shown in Fig. 2B, the intermolecular Σr^{-6} values, which are the sum of the inverse sixth power of the distances between each ligand proton and all receptor protons, in-

crease with an increase in the cube size, and converge for the total number of protons in the cube larger than 13^3. This means that additional protons in the cubes have negligible effects on the intermolecular saturation transfer rates. Therefore, to mimic the large receptors with a minimal number of protons, the total number of protons in the receptor cube is set to 13^3, as shown in Fig. 2C. Unless otherwise stated, the rotational correlation times of the ligand and the receptor molecules are set to 10 ns and 100 ns, respectively, which approximately correspond to molecular masses of 25 kDa and 250 kDa, respectively.

The best TCS experimental conditions are those where the L1 proton is most clearly discriminated from the L2 and L3 protons.

3.2. Effects of the proton concentration in the solvent

In the TCS method, a solvent with a low proton concentration is used to suppress the spin diffusion within the ligand molecules, by lowering the proton density in the ligand molecules. However, the low proton concentration in the solvent also reduces the observable magnetization by decreasing the proton occupancies of the exchangeable hydrogen sites in the ligand molecules. Therefore, it is important to determine the appropriate fractional proton concentration (p_{proton}) in the solvent for the TCS method.

The intensity ratios for the ligand protons calculated with various p_{proton}s are shown in Fig. 3. For the $p_{\text{proton}} = 100\%$, the intensity ratios of the three protons are almost indistinguishable from each other. However, with a decrease of p_{proton}, the intensity ratio of the L1 proton is more reduced and the intensity ratio of the L3 proton is less reduced, and for $p_{\text{proton}} = 10\%$, the L1 proton is clearly distinguishable from the L2 and the L3 protons. This is because the saturation transferred from the receptor protons to the L1 proton is further transferred to the L2 and/or L3 protons in the isotopomers with high proton densities, and the fractional populations of such isotopomers decrease at lower proton concentrations. Fig. 3G shows the intensity ratios calculated under the isolated spin pairs approximation (ISPsA) (Eq. (25)), corresponding to the condition where the p_{proton} is extremely low and the intra-ligand cross relaxation is negligible. A comparison of Figs. 3F and G reveals that the proton concentration of 10% gives an almost comparable result to that of ISPsA, which means that the spin diffusion is well suppressed by the proton concentration of 10% in this model spin system. Considering the trade-off between the degree of proton discrimination and the experimental sensitivity, $p_{\text{proton}} = 10$–30% is desirable.

3.3. Effects of kinetic parameters

As shown in Eq. (4), under the conditions mentioned above, the magnetizations of the ligand protons are affected by two parameters: the fractional population of the bound ligands, p_b, and the
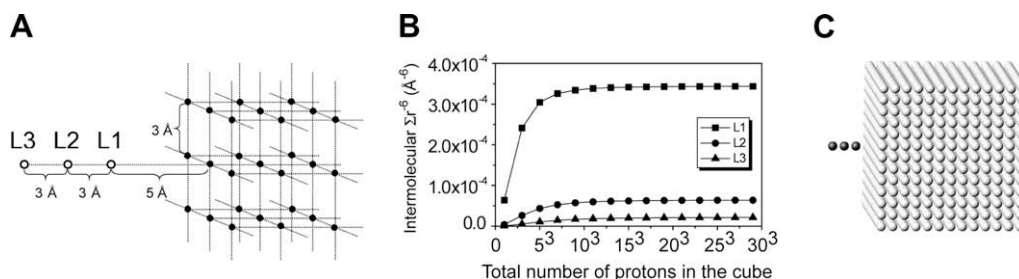

Fig. 2. Model spin system used in the simulation. (A) Basic structure of the model spin system. The ligand is composed of three exchangeable protons, L1, L2 and L3 (open circles) placed linearly with 3 Å spacing. The receptor is composed of non-exchangeable protons (closed circles) placed at 3 Å-spaced grid points in a cube. The distance between the L1 proton and the closest proton of the receptor is set to 5 Å. (B) The relationship between the total number of protons in the receptor and the intermolecular Σr^{-6} values for the ligand protons. (C) CPK model of the model spin system used in the simulation studies. The total number of protons in the receptor is 13^3. The ligand and receptor protons are gray and white, respectively.
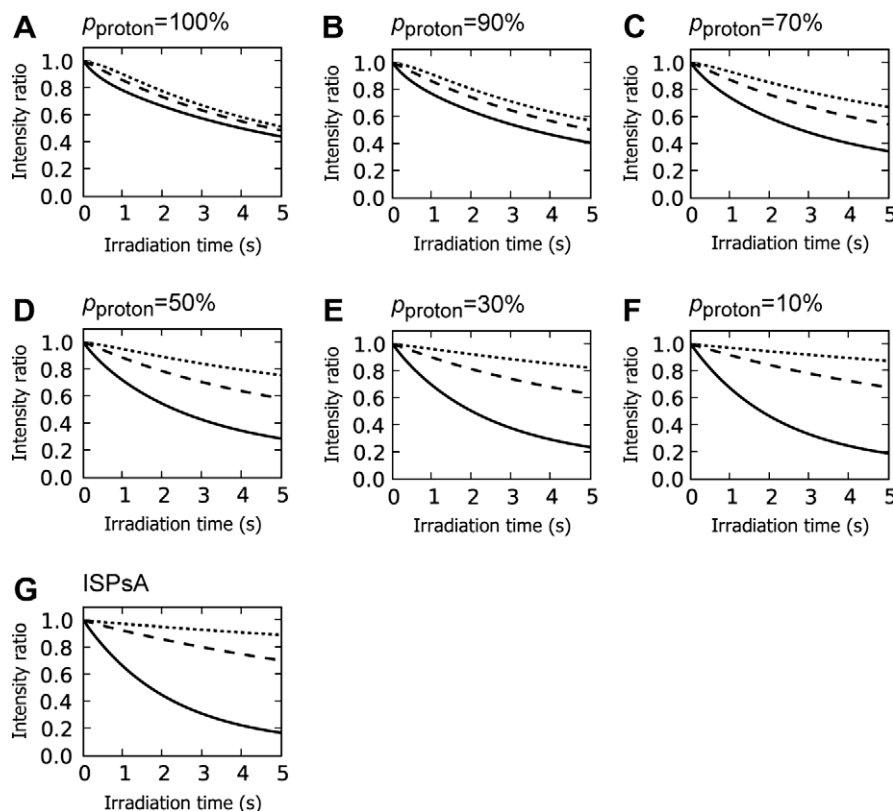
Fig. 3. Effects of the fractional proton concentration in the solvent (p_{proton}) on the signal intensity ratios. The signal intensity ratios for the L1, L2, and L3 protons are shown by the solid, dashed, and dotted lines, respectively. (A) $p_{\text{proton}} = 100\%$, (B) $p_{\text{proton}} = 90\%$, (C) $p_{\text{proton}} = 70\%$, (D) $p_{\text{proton}} = 50\%$, (E) $p_{\text{proton}} = 30\%$, (F) $p_{\text{proton}} = 10\%$, and (G) isolated spin pairs approximation (ISPsA).
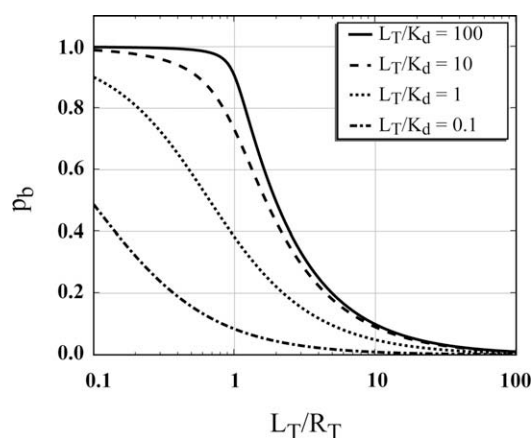

Fig. 4. Plot of the bound ligand fraction (p_b) as a function of L_T/R_T and L_T/K_d. The curves are calculated using Eq. (32).

dissociation rate constant, k_{off}. The p_b value can be controlled by adjusting the total ligand concentration L_T and the total receptor concentration R_T of the NMR samples according to the following equation:

$$p_b = \frac{[LR]}{L_T} = \frac{L_T + R_T + K_d - \sqrt{(L_T + R_T + K_d)^2 - 4L_T R_T}}{2L_T} \quad (32)$$

where $[LR]$ is the concentration of the complex, and K_d is the dissociation constant. Fig. 4 is a plot of the p_b values as a function of the L_T/R_T ratios and the L_T/K_d ratios. Fig. 4 indicates that, to achieve $p_b = 0.1$, the L_T/R_T ratio should be 10 for $L_T/K_d \geqslant 10$, the L_T/R_T ratio

should be 5 for $L_T/K_d = 1$, and the L_T/R_T ratio should be less than 1 for $L_T/K_d = 0.1$. Therefore, for low affinity interactions (high K_d), large L_T and R_T values are required to achieve high p_b. Because the L_T and R_T values are practically limited by the available amount and/or the solubility of the ligand and receptor, there are highest achievable p_b values, which determines the sensitivity of the TCS method (see below).

The intensity ratios for the ligand protons calculated with various p_bs and k_{off}s are shown in Fig. 5. Under the condition of $p_b = 0.01$, only a small reduction in the intensity ratios was observed within the rf-irradiation time of 5 s under any k_{off} values tested. However, the efficiency of the saturation is increased with the increase of p_b. For $k_{off} \geqslant 1$ s^{-1}, the L1 proton is clearly discriminated from the L2 and L3 protons, if $p_b \geqslant 0.1$. For $k_{off} \leqslant 1$ s^{-1}, the efficiency of the saturation is decreased with the decrease of k_{off}: for $k_{off} = 1$ s^{-1}, p_b should be larger than 0.1, and for $k_{off} = 0.1$ s^{-1}, the saturation transfer is not sufficient, even if $p_b = 0.5$.

To clarify the effect of p_b on the efficiency of the saturation, the concept of the average dwell time of the ligands in the bound state during rf-irradiation ($\overline{T_{bound}}$) is introduced. $\overline{T_{bound}}$ is given by

$$\overline{T_{bound}} = N_{turnover} \cdot \tau_{bound} \cdot T_{irrad} \quad (33)$$

where τ_{bound} is the average dwell time of the ligands in the bound state during a single turnover, T_{irrad} is the duration of the rf-irradiation, and N_{turnover} is the average number of the "turnover" events per second. The "turnover" is defined as the process where the ligands experience one cycle of association and dissociation.

The average dwell times of the ligands in the free and bound states during a single turnover, τ_{free} and τ_{bound}, respectively, are given by the inverse of the association rate and the dissociation rate, respectively.
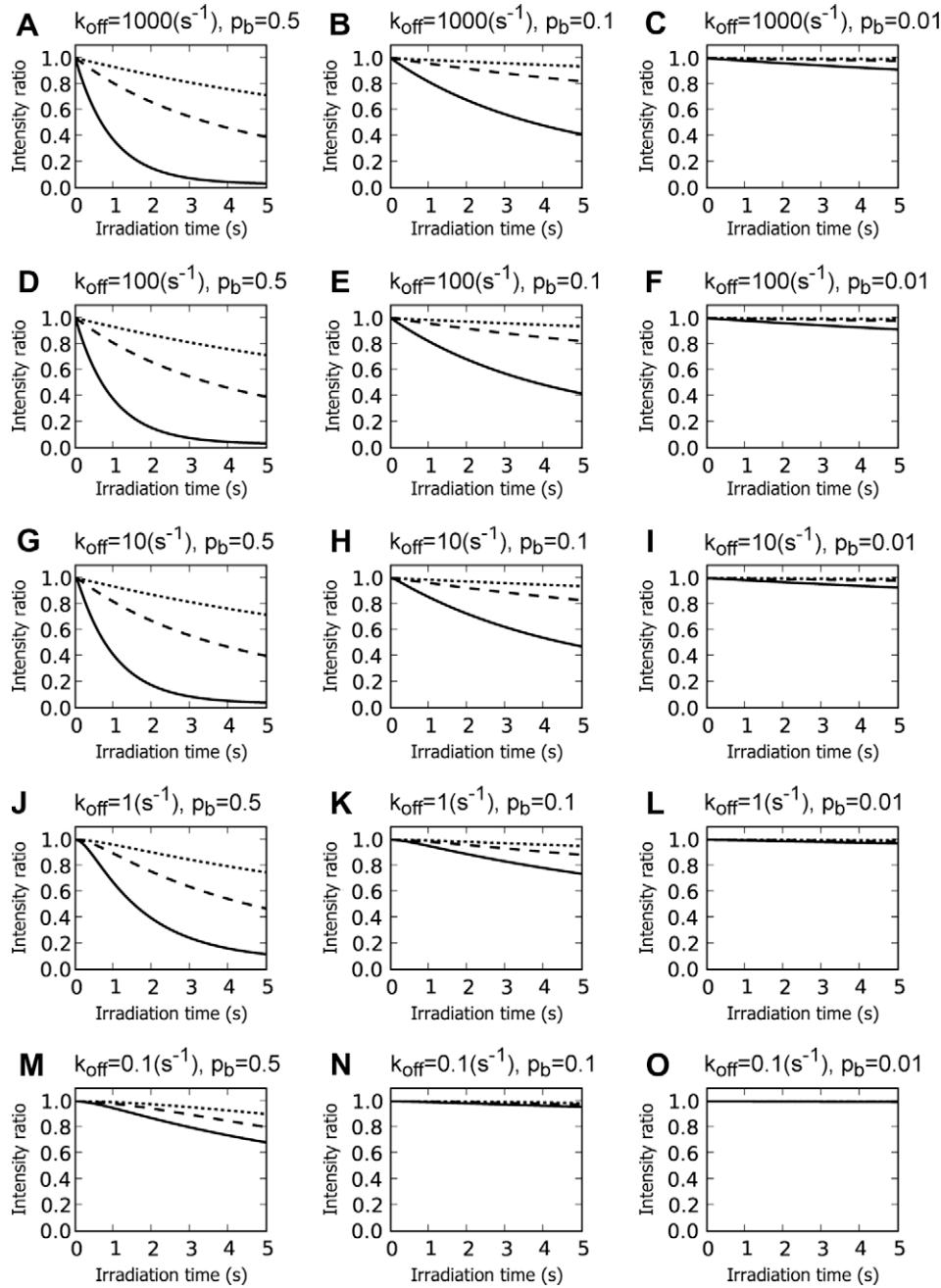
Fig. 5. Effects of the bound ligand fraction (p_b) and the dissociation rate constant (k_{off}) on the signal intensity ratios. Signal intensity ratios were calculated under the condition of $\tau_{c,L}$ = 10 ns, $\tau_{c,R}$ = 100 ns and a 10% fractional proton concentration. The signal intensity ratios for the L1, L2, and L3 protons are shown by the solid, dashed, and dotted lines, respectively. (A)–(C) k_{off} = 1000 s^{-1} (A) p_b = 0.5 (B) p_b = 0.1 (C) p_b = 0.01 (D)–(F) k_{off} = 100 s^{-1} (D) p_b = 0.5 (E) p_b = 0.1 (F) p_b = 0.01 (G)–(I) k_{off} = 10 s^{-1} (G) p_b = 0.5 (H) p_b = 0.1 (I) p_b = 0.01 (J)–(L) k_{off} = 1 s^{-1} (J) p_b = 0.5 (K) p_b = 0.1 (L) p_b = 0.01 (M)–(O) k_{off} = 0.1 s^{-1} (M) p_b = 0.5 (N) p_b = 0.1 (O) p_b = 0.01.

$$\tau_{free} = \frac{1}{k_{on}[R]} = \frac{1 - p_b}{p_b k_{off}} \qquad (34)$$

$$\tau_{bound} = \frac{1}{k_{off}} \qquad (35)$$

The average time for one "turnover" event ($\tau_{turnover}$) is the sum of τ_{free} and τ_{bound}, and $N_{turnover}$ is given by the inverse of $\tau_{turnover}$.

$$N_{turnover} = \frac{1}{\tau_{turnover}} = \frac{1}{\tau_{free} + \tau_{bound}} = p_b k_{off} \qquad (36)$$

Therefore, from Eq. (33) $\overline{T_{bound}}$ is given by

$$\overline{T_{bound}} = p_b T_{irrad} \qquad (37)$$

Therefore, p_b proportionally affects the $\overline{T_{bound}}$, which is consistent with the increase in the efficiency of the saturation with increasing p_b in Fig. 5. A similar p_b-dependency was previously reported for trNOE [16].

Eq. (36) demonstrates that p_b and k_{off} determine the "turnover" rate. To further understand how p_b and k_{off} affect the sensitivity of the TCS method, the total time that each ligand molecule spends in the bound state during the rf-irradiation periods was statistically analyzed. Hereafter, this value is referred to as the "effective saturation time" (EST). Since the each ligand molecule stochastically repeats the exchange between the free and bound states during the
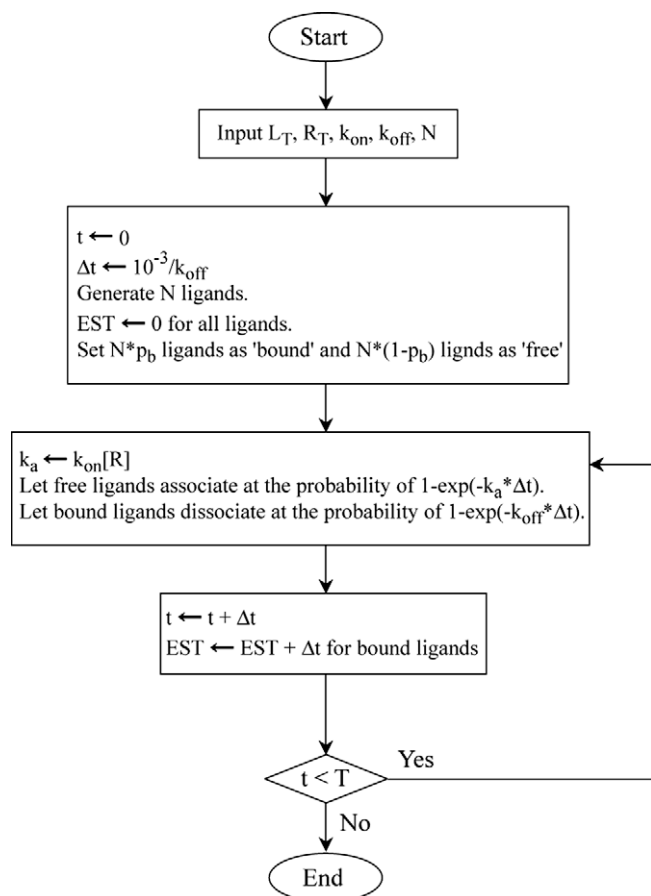
Fig. 6. Simulation protocol to calculate the distribution of the "effective saturation time" (EST).

rf-irradiation period, the ESTs are neither necessarily equal to $\overline{T_{bound}}$ nor continuously increased with the evolution of the irradiation time. The simulated ESTs are calculated by virtually letting the association and dissociation happen as probabilistic events for 10,000 virtual ligand molecules (see Section 5 and Fig. 6). The distributions of the simulated ESTs are shown in Fig. 7. For $p_b = 0.5$ and 0.1 (Fig. 7B–D and F–H), the distributions of ESTs are symmetrical and centered at $\overline{T_{bound}}$. However, for $p_b = 0.01$ (Fig. 7J–L), the distributions of ESTs are asymmetrical, and after 1 s and 3 s of the rf-irradiation, ESTs of 38% and 5.6% of the ligands remain at 0 s, which means that those ligands do not form a complex with the receptors during the rf-irradiation periods, due to the small $N_{turnover}$ (small p_b and/or small k_{off} values).

3.4. Effects of the molecular weight of the receptor

The TCS method is applicable to a system where the molecular weight of the receptors is large. Theoretically, as the rotational correlation times of the receptor, $\tau_{c,R}$, increases, the relaxation rates due to ^1H–^1H dipole–dipole interaction in the bound state increase. Therefore, as $\tau_{c,R}$ increases, ρ_b and $\sum_i^{receptor} \sigma_i$ increase, and the efficiency of saturation (Eq. (27)) and the initial decay rate (Eq. (28)) increase. To evaluate the effect of the molecular weight of the receptors on the observed TCS effects, we calculated the signal intensity ratios by setting $\tau_{c,R}$ to 10 ns, 100 ns, and 1000 ns, which approximately correspond to molecular masses of 25 kDa, 250 kDa, and 2500 kDa, respectively.

As shown in Fig. 8, as $\tau_{c,R}$ increases, the efficiency of the saturation also increases. For $\tau_{c,R} = 100$ ns, a reduction of the signal inten-

sity ratios that is large enough to identify the binding interface is observed for $p_b = 0.5$ and 0.1. However, for $\tau_{c,R} = 10$ ns, large reductions of the intensity ratios are not observed for $p_b = 0.1$. For $\tau_{c,R} = 1000$ ns, it is preferable to use $p_b = 0.1$ or 0.01, or $p_b = 0.5$ and an irradiation time shorter than 0.5 s. Based on these results, we conclude that the TCS method is applicable to a receptor with a rotational correlation time of 10–1000 ns, and that the lower limit of p_b decreases as the molecular weight of the receptor increases.

3.5. Experimental verification of the TCS simulation

In the theoretical description of the TCS experiments, we made the following assumptions for simplification: (i) receptor protons are instantaneously saturated, (ii) ligand proton magnetizations recover their equilibrium state during the interscan delay, (iii) aliphatic protons in ligands are completely deuterated, and (iv) longitudinal relaxation of ligand protons, due to ^1H–^2H dipole–dipole interactions, H–D exchange, or paramagnetic relaxation is negligible [17]. In the model spin simulation, we also assumed that the model spin system sufficiently mimics the spatial configuration of protons in protein–protein complexes. Therefore, these assumptions were experimentally verified, using the known structure of the complex of ubiquitin and yeast ubiquitin hydrolase 1 (YUH1) [18].

The TCS experiments were performed, using unlabeled YUH1 and uniformly $^2H,^{15}N$-labeled ubiquitin. To achieve the instantaneous saturation of YUH1, the experiments were performed at a low temperature (10 °C). TRACT experiments revealed that the τ_c of the ubiquitin–YUH1 complex determined at 10 °C is 27 ns, which corresponds to that of a ∼50 kDa protein at room temperature [19]. Fig. 9A–C show that intensity ratios of the ubiquitin residues, G47 and S20, under various conditions. G47 and S20 are located in close proximity to YUH1 and away from YUH1, respectively (Fig. 9D). The TCS experiments in Fig. 9A were performed under the empirically optimized experimental conditions with a ubiquitin/YUH1 ratio = 4:1. In Fig. 9B, the concentration of YUH1 was lower than that in Fig. 9A (ubiquitin/YUH1 ratio = 10:1) [20]. In Fig. 9C, the ubiquitin/YUH1 ratio was the same as that in Fig. 9A, but the YUH1 C90S mutant, which dissociates from ubiquitin more slowly than wild type YUH1, was used instead of wild type YUH1. In Fig. 9A, the resonance from G47 was ∼30% affected by a one second irradiation. On the other hand, in Figs. 9B and C, the corresponding intensity ratios were only 13% and <10%, respectively. In all of the experiments, the intensity ratios of the resonances from S20 were <5%.

Subsequently, we carried out the model spin simulation under the corresponding conditions. Fig. 9D–F show the calculated intensity ratios under the conditions similar to those of Fig. 9A–C, respectively, using the model spin system with Σr^{-6} of L1 equal to that of the G47 amide proton in the ubiquitin–YUH1 complex. As a result, the intensity ratios of L1 in Fig. 9D–F were similar to those of G47 in Fig. 9A–C, suggesting that the assumptions were valid under the present experimental conditions, and the simulation was effective for the optimization of the TCS experimental conditions.

4. Conclusion

In this paper, we formulated the behavior of the observable magnetizations in the TCS method by explicitly incorporating isotopomers in the sample solution, and by making several assumptions, we developed a simplified theory for the TCS method. We estimated the effect of each experimental parameter on the observed signal intensities by simulation studies, using the simplified theory. Based on these results, we proposed guidelines for setting
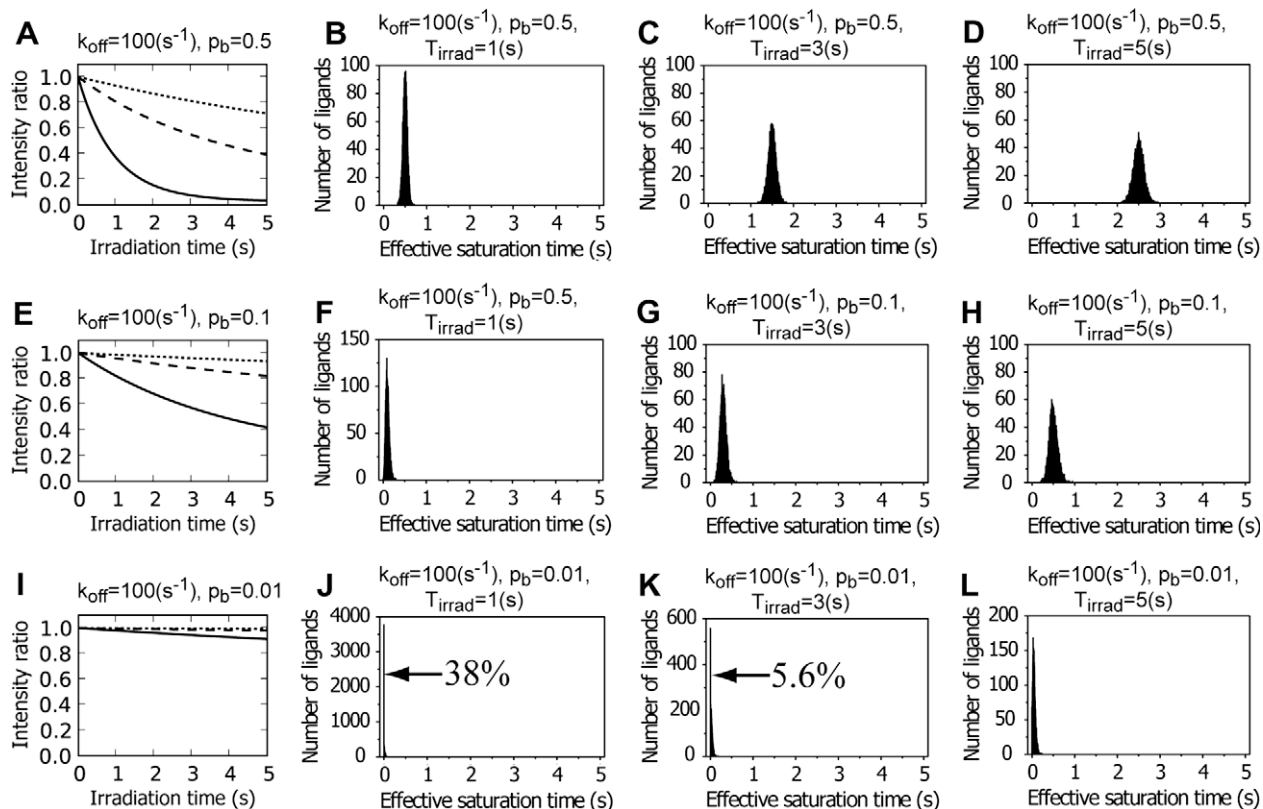
Fig. 7. Effects of the bound ligand fraction (p_b) on the "effective saturation time" (ESTs). The distribution of ESTs calculated for 10,000 virtual ligands is shown with k_{off} = 100 s^{-1} and p_b = 0.5 (B–D), p_b = 0.1 (F–H) and p_b = 0.01 (J–L), respectively. (B), (F), (J) T_{irrad} = 1 s (C), (G), (K) T_{irrad} = 3 s (D), (H), (L) T_{irrad} = 5 s (A), (E), (I) Signal intensity ratios calculated under the conditions of $\tau_{c,L}$ = 10 ns, $\tau_{c,R}$ = 100 ns, k_{off} = 100 s^{-1} and a 10% fractional proton concentration are shown with p_b = 0.5, p_b = 0.1 and p_b = 0.01, respectively. The signal intensity ratios for the L1, L2, and L3 protons are shown by the solid, dashed, and dotted lines, respectively.
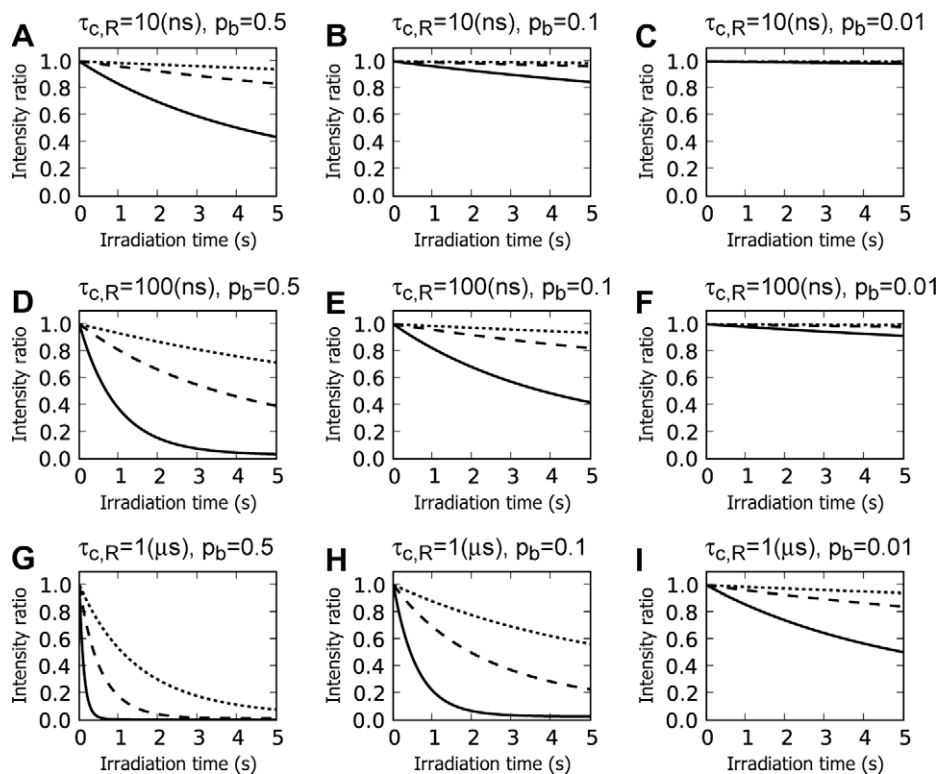

Fig. 8. Effects of the bound ligand fraction (p_b) and the rotational correlation times of receptors ($\tau_{c,R}$) on the signal intensity ratios. Signal intensity ratios for the protons L1, L2, and L3 are shown by solid, dashed, and dotted lines, respectively. (A)–(C) $\tau_{c,R}$ = 10 ns (A) p_b = 0.5 (B) p_b = 0.1 (C) p_b = 0.01 (D)–(F) $\tau_{c,R}$ = 100 ns (D) p_b = 0.5 (E) p_b = 0.1 (F) p_b = 0.01 (G)–(I) $\tau_{c,R}$ = 1000 ns (G) p_b = 0.5 (H) p_b = 0.1 (I) p_b = 0.01.
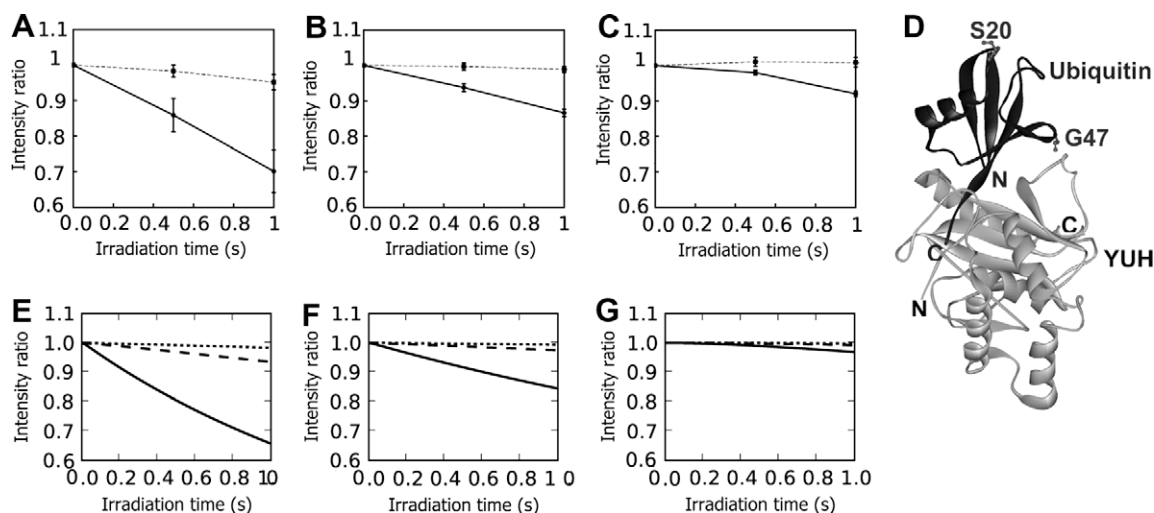
Fig. 9. Comparison of the experimentally observed intensity ratios and the calculated intensity ratios. (A–C) Experimentally observed signal intensity ratios of ubiquitin G47, which is in close proximity to YUH1 (solid lines), and ubiquitin S20, which is away from the YUH1 protons (dashed lines), in the TCS experiments of the ubiquitin–YUH1 interaction under various conditions: (A) empirically optimized condition with ubiquitin/YUH1 ratio = 4:1, (B) ubiquitin/YUH1 ratio = 10:1, and (C) ubiquitin/YUH1 ratio = 4:1 but with the YUH C90S mutant, which dissociates from ubiquitin more slowly than the wild type. (D) Location of the ubiquitin G47 and S20 residues in the structure of the ubiquitin–YUH1 complex (PDB ID: 1CMX). (E–G) calculated signal intensity ratios in the model spin simulations under the conditions corresponding to (A), (B), and (C), respectively. The molecular diagram was generated by WebLab Viewer Pro (Molecular Simulations, Inc.).

up the optimal experimental conditions for TCS experiments. The proposed guidelines were verified by the TCS experiments for the interaction between ubiquitin and YUH1. The established theory will enable us to analyze the observed TCS effect quantitatively and obtain the inter molecular distance information for large protein complexes.

5. Materials and methods

5.1. Simulation of the TCS experiments

Intensity ratios were calculated according to Eq. (26) with $M_f(t)$ in Eq. (3), except for Fig. 3G, where $M_f(t)$ in Eq. (28) was used. The Larmor frequency for ^1H was fixed to 600 MHz. The rotational correlation time for the complex ($\tau_{c,LR}$) was treated as the sum of those for the free ligand ($\tau_{c,L}$) and the free receptor ($\tau_{c,R}$). All of the calculations were performed by an in-house developed computer program, written in Python 2.5 or in Java.

5.2. Protocol to calculate the simulated distribution of "effective saturation time"(EST)

The protocol to calculate the simulated distribution of "effective saturation time" is depicted in Fig. 6. In Step 1, L_T, R_T, k_{on}, k_{off}, N (the number of virtual ligands) and T (the duration of simulation) are inputted. In this paper, N and T were fixed at 10,000 and 5, respectively. In Step 2, the system time, t, is set to 0, and the increment size of the system time, Δt, is set to $10^{-3}/k_{off}$. Then the N virtual ligands are generated and their ESTs are set to zero, the $p_b * N$ ligands are set as "bound" and the $(1 - p_b) * N$ ligands are set as "free", to virtually equilibrate the system. In Step 3, the association rate constant, k_a, is calculated from k_{on} and [R]. Then, the free ligands are allowed to associate at a probability of $1 - \exp(-k_a * \Delta t)$, and the bound ligands are set to dissociate at a probability of $1 - \exp(-k_{off} * \Delta t)$. In Step 4, the system time, t, and ESTs of bound ligands are increased by Δt. In Step 5, the system time is increased by Δt, and Steps 3–5 are repeated while $t < T$.

5.3. TCS experiments

Uniformly $^2H,^{15}N$-labeled Ub was over-expressed by growing *Escherichia coli* BL21 (DE3) (Novagen), containing the plasmid encoding ubiquitin (pET26b/ubiquitin), in M9 medium with 1.0 g of ^{15}N-labeled ammonium chloride, 2.0 g of D-glucose-d$_6$, and 1.0 g of $^2H,^{15}N$-Celtone Base powder in 1 L ^2H_2O. Protein purification was performed, according to the previous report [21]. The wild type and C90S mutant of YUH1 were over-expressed in LB medium and purified as previously described [20].

The NMR experiments were carried out at 10 °C in 50 mM sodium phosphate, pH 6.0, 100 mM NaCl, and 20%H$_2$O/80% D$_2$O with a Bruker Avance 500 spectrometer equipped with a cryogenic probe. In the TCS experiments, 200 μM uniformly ^2H, ^{15}N labeled ubiquitin was combined with 50 or 20 μM unlabeled YUH1. The pulse scheme was described previously [22]. The irradiation frequency was set at −0.5 ppm, and the maximum radiofrequency amplitude was 0.21 kHz for WURST-2 (the adiabatic factor Q_0 = 1) [23]. The irradiation time was set to either 0.5 or 1 s, and the total recycling delay was set to 6.0 s. The total experimental time was 20 h for each sample condition. All of the recorded spectra were processed by Topspin 2.0 (Bruker), and were analyzed by Sparky (Goddard T. D., and Kneller D. G., SPARKY 3, University of California, San Francisco).

5.4. Model spin simulation under the experimental conditions

The simulations were carried out using the model spin system in Fig. 1, with the distance between the ligand proton L1 and the closest proton of the receptor modified from 5.0 to 3.75 Å. $\tau_{c,L}$ and $\tau_{c,R}$ were set to 5.4 and 27 ns, respectively, based on the TRACT experiments (data not shown) [19]. The dissociation rates (k_{off}) of the wild type and C90S mutant YUH1 were set to 100 and 0.2 s^{-1} respectively, based on the line shape analysis [24] and the TROSY ZZ-exchange experiments [25] (data not shown). p_b was calculated from the dissociation constant (K_d) and the concentrations of ubiquitin and YUH1. The values K_d of the wild type and C90S mutant YUH1 were set to 18 μM and 37 nM, respectively [20,21]. Under the conditions employed (200 μM ubiquitin and 50 or 20 μM YUH1), >90% of YUH1 is bound to ubiquitin.

Acknowledgments

References

[1] T. Nakanishi, M. Miyazawa, M. Sakakura, H. Terasawa, H. Takahashi, I. Shimada, Determination of the interface of a large protein complex by transferred cross-saturation measurements, J. Mol. Biol. 318 (2002) 245–249.

[2] K. Takeuchi, M. Yokogawa, T. Matsuda, M. Sugai, S. Kawano, T. Kohno, H. Nakamura, H. Takahashi, I. Shimada, Structural basis of the KcsA K(+) channel and agitoxin2 pore-blocking toxin interaction by using the transferred cross-saturation method, Structure 11 (2003) 1381–1392.

[3] M. Yokogawa, K. Takeuchi, I. Shimada, Bead-linked proteoliposomes, J. Am. Chem. Soc. 127 (2005) 12021–12027.

[4] N. Nishida, H. Sumikawa, M. Sakakura, N. Shimba, H. Takahashi, H. Terasawa, E. Suzuki, I. Shimada, Collagen-binding mode of vWF-A3 domain determined by a transferred cross-saturation experiment, Nat. Struct. Biol. 10 (2003) 53–58.

[5] O. Ichikawa, M. Osawa, N. Nishida, N. Goshima, N. Nomura, I. Shimada, Structural basis of the collagen-binding mode of discoidin domain receptor 2, EMBO J. 26 (2007) 4168–4176.

[6] Y. Kofuku, C. Yoshiura, T. Ueda, H. Terasawa, T. Hirai, S. Tominaga, M. Hirose, Y. Maeda, H. Takahashi, Y. Terashima, K. Matsushima, I. Shimada, Structural basis of the interaction between chemokine stromal cell-derived factor-1/CXCL12 and its G-protein-coupled receptor CXCR4, J. Biol. Chem. 284 (2009) 35240–35250.

[7] K. Takeuchi, H. Takahashi, M. Sugai, H. Iwai, T. Kohno, K. Sekimizu, S. Natori, I. Shimada, Channel-forming membrane permeabilization by an antibacterial protein, sapecin, J. Biol. Chem. 279 (2004) 4981–4987.

[8] P. Balaram, A.A. Bothner-By, J. Dadok, Negative nuclear Overhauser effects as probes of macromolecular structure, J. Am. Chem. Soc. 94 (1972) 4015–4017.

[9] R. Noyori, Y. Kumagai, I. Umeda, H. Takaya, Localization of tyrosine at the binding site of neurophysin II by negative nuclear Overhauser effects, J. Am. Chem. Soc. 94 (1972) 4017–4020.

[10] M. Mayer, B. Meyer, Characterization of ligand binding by saturation transfer difference NMR spectroscopy, Angew. Chem., Int. Ed. Engl. 38 (1999) 1784–1788.

[11] G.M. Clore, A.M. Gronenborn, Theory and applications of the transferred nuclear Overhauser effect to the study of the conformations of small ligands bound to proteins, J. Magn. Reson. 48 (1982) 402–417.

[12] G.M. Clore, A.M. Gronenborn, Theory of the time-dependent transferred nuclear Overhauser effect – applications to structural-analysis of ligand protein complexes in solution, J. Magn. Reson. 53 (1983) 423–442.

[13] V. Jayalakshmi, N.R. Krishna, Complete relaxation and conformational exchange matrix (CORCEMA) analysis of intermolecular saturation transfer effects in reversibly forming ligand–receptor complexes, J. Magn. Reson. 155 (2002) 106–118.

[14] Z. Zolnai, N. Juranic, S. Macura, Full matrix analysis of cross-relaxation fails in fractionally deuterated molecules, J. Biomol. NMR 12 (1998) 333–337.

[15] M. Goldman, Quantum description of high-resolution NMR in liquids, Clarendon Press, 1988. ISBN 019855639X.

[16] A.P. Campbell, B.D. Sykes, Theoretical evaluation of the 2-dimensional transferred nuclear Overhauser effect, J. Magn. Reson. 93 (1991) 77–92.

[17] T.S. Ulmer, I.D. Campbell, J. Boyd, Amide proton relaxation measurements employing a highly deuterated protein, J. Magn. Reson. 166 (2004) 190–201.

[18] S.C. Johnston, S.M. Riddle, R.E. Cohen, C.P. Hill, Structural basis for the specificity of ubiquitin C-terminal hydrolases, EMBO J. 18 (1999) 3877–3887.

[19] D. Lee, C. Hilty, G. Wider, K. Wuthrich, Effective rotational correlation times of proteins from NMR relaxation interference, J. Magn. Reson. 178 (2006) 72–76.

[20] J. Moriya, M. Sakakura, Y. Tokunaga, R.S. Prosser, I. Shimada, An NMR method for the determination of protein binding interfaces using TEMPOL-induced chemical shift perturbations, Biochim. Biophys. Acta 1790 (2009) 1368–1376.

[21] T. Sakamoto, T. Tanaka, Y. Ito, S. Rajesh, M. Iwamoto-Sugai, Y. Kodera, N. Tsuchida, T. Shibata, T. Kohno, An NMR analysis of ubiquitin recognition by yeast ubiquitin hydrolase, Biochemistry 38 (1999) 11634–11642.

[22] H. Takahashi, T. Nakanishi, K. Kami, Y. Arata, I. Shimada, A novel NMR method for determining the interfaces of large protein–protein complexes, Nat. Struct. Biol. 7 (2000) 220–223.

[23] E. Kupce, G. Wagner, Wideband homonuclear decoupling in protein spectra, J. Magn. Reson. Ser. B 109 (1995) 329–333.

[24] G.S. Huang, T.G. Oas, Submillisecond folding of monomeric lambda repressor, Proc. Natl. Acad. Sci. USA 92 (1995) 6878–6882.

[25] D. Sahu, G.M. Clore, J. Iwahara, TROSY-based z-exchange spectroscopy, J. Am. Chem. Soc. 129 (2007) 13232–13237.